Carbohydrate Polymers 75 (2009) 369–379

Contents lists available at ScienceDirect

Carbohydrate Polymers

journal homepage: www.elsevier.com/locate/carbpol

Review

NMR spectroscopy and imaging studies of pharmaceutical tablets made of starch

Héloïse Thérien-Aubin, X.X. Zhu *

Département de Chimie, Université de Montréal, C.P. 6128, Succ. Centre-ville, Montréal, QC., Canada H3C 3J7

ARTICLE INFO

Article history:
Received 27 May 2008
Received in revised form 7 August 2008
Accepted 13 August 2008
Available online 20 August 2008

Keywords:
Starch
Drug release
NMR imaging
^{13}C CP/MAS NMR spectroscopy

ABSTRACT

Modified polysaccharides such as high amylose starch are used as excipient in controlled drug release technology. Crosslinked high amylose starch is a hydrophilic matrix used for the sustained release of drugs. Tablets using modified hybrid starch as excipient display zero-order release over 2–24 h. A release over 3–4 weeks was observed when the modified starch is used as an implant. The use of starch in controlled release system is appealing because it could be easily metabolized in the human body. We review here the use of NMR imaging and solid state ^{13}C spectroscopy in the study of the various factors influencing drug release in such systems.

1. Introduction

1.1. Starch structure

Starch is a mixture of two natural polymers, amylose and amylopectin (Whistler, BeMiller, & Paschall, 1984). Those two polymers are composed of D-glucoyranose molecules linked by an acetal bond at the α-1,4 position. Amylose is a linear polymer made up of 250–5000 glucose units. Amylopectin, in contrast, is a slightly branched polymer of high molecular weight made up of 10,000–100,000 glucose units. In amylopectin, in addition to the α-1,4 linkage of amylose, 2–5% of branched points are present through α-1,6 acetal bonding (Robyt, 1998). This branching results in the cluster structure adopted by amylopectin. Each branch of amylopectin is composed of 20–30 glucose units. The resulting structure is flexible enough to allow the crystallization of amylopectin, an unusual properties for branched polymers.

Natural and chemically-modified starches can adopt a variety of crystalline structures. The preferred crystalline structure of a starch sample depends on both the amylopectin structure and the ratio amylose/amylopectin (Barsby, Donald, & Frazier, 2001). Consequently, the crystalline structure observed is highly dependent on the biological origin of the starch granule. The crystalline structures of the starch could be observed by X-ray diffraction and ^{13}C CP/MAS NMR spectroscopy (Fig. 1) (Buleon, Colonna, Planchot, & Ball, 1998; Gidley & Bociek, 1985, 1988).

Cereal starch, from corn, wheat or rice, typically adopts an A-type crystalline structure. This type of crystalline structure is favored by amylopectin having short lateral chains and branching points close to each other (Barsby et al., 2001). Fruit and tuber starches have a different crystalline structure, the B-type, favored by long side chains and distant branching points (Buleon et al., 1998). C-type crystalline structure was observed in leguminous plant. This type of starch is in fact a mixture of A and B-type crystalline structure. In peas, for example, starch in the center of the granule adopts a B-type crystalline structure while the periphery of the granule is composed of A-type structures (Bogracheva, Morris, Ring, & Hedley, 1998). Starch could also adopt a V-type crystalline structure (from Verkleisterung derived from the German word Kleister meaning 'gelatinized starch') (Whistler et al., 1984). This crystalline structure is usual of modified starch, but is also observed in the endosperm of some native starch granule. Formation of inclusion complexes between amylose and fatty acids, water, alcohol, iodine or other small molecules gives rise to the formation of V-type crystalline structure. V-type structure is also formed when cooling a starch solution previously heated to a temperature above its gelatinization temperature in the presence of a molecule to complex (Bulpin, Welsh, & Morris, 1982).

The structures of A- and B-types of crystalline starch are similar. They are both formed by the packing of double helices of amylose and amylopectin. The V-type crystalline structure, however, is composed of single helices. V-type helices are composed by six glucose units by turn (Fig. 2A), and the helix pitch is 0.8 nm (Immel & Lichtenthaler, 2000). The hollow structure in the helix is large enough to accommodate small molecules, which could lead to the formation of inclusion complexes. A- and B-type double helices are composed of two times six glucose units by turn and the helix pitch is longer than V-type helix (Fig. 2B), i.e. 2.1 nm (Imberty, Buleon, Vinh, & Perez, 1991; Wu & Sarko, 1978a, 1978b). In A-type crystalline domains, the double helices are packed in a monoclinic cell (Imberty, Chanzy, Perez, Buleon, & Tran, 1988; Imberty et al.,

* Corresponding author.
E-mail address: julian.zhu@umontreal.ca (X.X. Zhu).

0144-8617/$ - see front matter © 2008 Elsevier Ltd. All rights reserved.
doi:10.1016/j.carbpol.2008.08.010

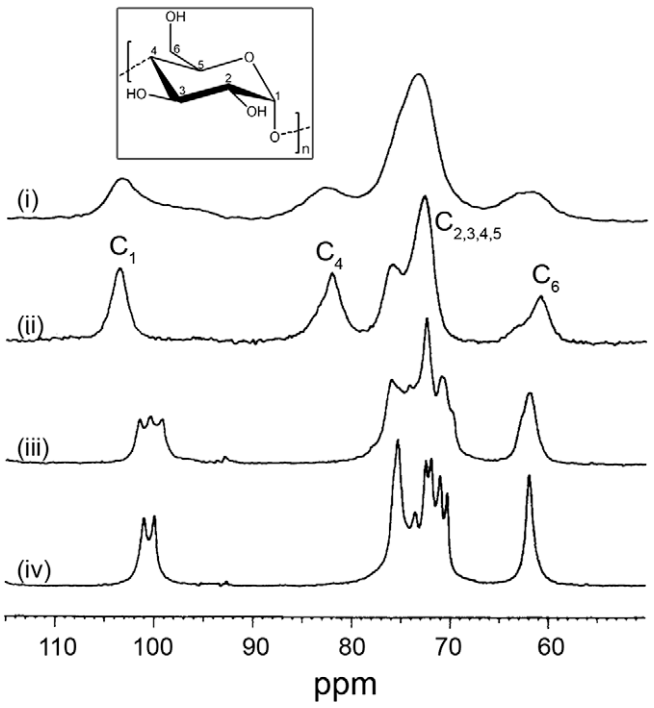

Fig. 1. ^{13}C CP/MAS NMR spectrum obtained at 75.46 MHz with a contact time of 1 ms of (i) amorphous starch, and (ii) V-type, (iii) A-type, (iv) B-type crystalline structure. Reprint from Gidley et al. (Gidley & Bociek, 1988) with the permission of the American Chemical Society. The inset represents the chemical structure of α(1–4)glucopyranose repeating unit of starch with $^4C_1$ chair conformation.

1991), where each helix has six neighboring helices, in a B-type crystalline domains the double helices are packed in a hexagonal cell with three neighboring helices (Imberty et al., 1991). The density of A-type crystalline domains is higher than that of the B-type domains mainly because of the closer packing of the helices.

1.2. Thermal transitions of starch

Starch gelatinization reefers to the irreversible endothermic transition associated with the loss of crystalline domains and lamellar structure of the starch granule (Barsby et al., 2001). When a water suspension of starch granule is heated, water will diffuse inside the granule which will swell the granule, heat will then break the hydrogen bonds which maintain the structural integrity of the starch granules. The gelatinization leads to the segregation of the amylose chains and the amylopectin clusters leading to an increase of local viscosity of the starch suspension. The gelatinization temperature of a starch sample will vary according to the number of glucose units implicated in the formation of helices, i.e. the size of the crystalline domains. An increased number of glucose units will lead to an increase in the gelatinization temperature. The gelatinization temperature is usually observed between 50 and 110 °C (Barsby et al., 2001), but also at lower temperatures in highly alkaline media. The use of starch as a thickener usually involves starch gelatinization.

Starch retrogradation is an exothermic transition which is characterized by the aggregation and crystallization of starch chains in gels. Classically, starch retrogradation is associated with an increased stiffness of the sample (Miles, Morris, Orford, & Ring, 1985). Upon retrogradation of highly concentrated starch solution, the formation of a rigid tridimensional network is observed (Gidley, 1989). Bread stalling is a common example of starch retrogradation (Morgan, Furneaux, & Stanley, 1992).

1.3. High amylose starch

In the 1940's a recessive gene leading to the production of a starch enriched in amylose was identified in different varieties of corn. This discovery led to the creation of corn producing starch with a content of 50%, 70%, and even 90% of amylose (Whistler et al., 1984). Properties of high amylose starch from a given botanical sources differs from the 'normal' starches of the same botanical source richer in amylopectin. In high amylose starch, the gelatinization temperature is higher (Whistler et al., 1984), the range covered by this transition is wider (Shi, Capitani, Trzasko, & Jeffcoat, 1998), the granule swelling is reduced (Whistler et al., 1984), the gels formed by high amylose starch are more rigid (Case et al., 1998) and the effect of amylase enzyme is reduced. The crystalline degree of high amylose starch is also lower (Morrison, Tester, & Gidley, 1994; Shi et al., 1998).

The differences observed between 'normal' starches and high amylose starches are not only related to the different amylose/amylopectin ratio, but also to different amylopectin architecture (Shi et al., 1998). High amylose corn starch treated with isoamylase, an enzyme that specifically cleave the α-1,6 bonding, shows that the proportion of long side chains is higher than in 'normal' corn starch. Because of this uncommon architecture, high amylose corn starch adopts preferentially a crystalline structure of B-type while 'normal' corn starch shows a A-type crystalline structure (Shi et al., 1998; Whistler et al., 1984).

2. Crosslinked high amylose starch excipient for controlled drug release

The use of native starch as excipient is limited due to its low compressibility leading to the formation of weak tablets subject to capping (Rowe, Sheskey, & Weller, 2003). Chemical modifications of starch led to the development of more versatile excipients (Cartilier, Ungur, & Chebli, 2006; Chebli, Moussa, Buczkowski, & Cartilier, 1999; Dumoulin, Carriere, & Ingenito, 1998b; Joensson, Gustavsson, Laakso, & Reslow, 2002; Lefevre, Fuertes, & Quettier, 2001; Lenaerts, Chouinard, Mateescu, & Ispas-Szabo, 2002; Lenaerts, Dumoulin, & Mateescu, 1991; Lenaerts et al., 1998, 2003; Mateescu, Lenaerts, & Dumoulin, 1992; Pope & Royce, 1987; Rudnic, McCarty, & Belenduik, 1996; Te Wierik, Eissens, Bergsma, Arends-Scholte, & Lerk, 1997; Zhang, Xiao, Bindzus, & Green, 2006). Among the different chemical modifications, crosslinking is the more common. Epichlorohydrin is a widely used crosslinking agent (Cartilier et al., 2006; Lenaerts et al., 1991; Mateescu et al., 1992). However, epichlorohydrin is toxic and carcinogenic, (O'Neil, 2006) driving the pharmaceutical and food industries to use less toxic crosslinking agents (Lenaerts et al., 2003) such as sodium trimethaphosphate or phosphorus oxychloride (Dumoulin et al., 1998b; Lefevre et al., 2001; Lenaerts et al., 2003).

Two types of crosslinked high amylose starch (CHAS) excipient (Fig. 3) were studied by ^{13}C NMR spectroscopy and NMR imaging. Difference in swelling, water uptake, and drug release is observed between the tablets made of two types of CHAS powder, CHAS I swells more and faster than CHAS II leading to a faster water uptake and a faster drug release.

In both preparation methods, the crosslinking step is essential to improve the stability and the toughness of the starch gels formed upon hydration. The instability is often associated with the retrogradation of the starch, both the crosslinking and the functionalization will limit the reorganization of the starch chains leading to retrogradation. Crosslinks hinder the movement of the starch chains thus limiting the retrogradation (Ravenelle & Rahmouni, 2006; Whistler et al., 1984). The gelatinization step is essential to increase the hydrophilicity of the final excipient.

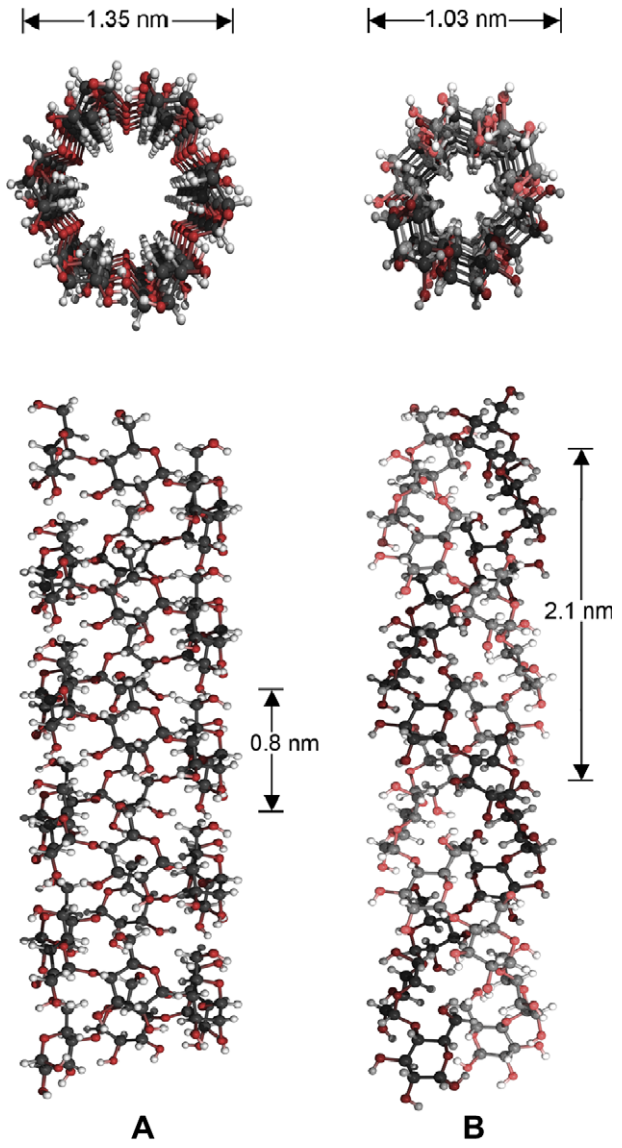

Fig. 2. Helical structure of crystalline starch. (A) V-type single helix. (B) A-type double helix. Drawn according to the crystalline structure of Immel et al. (Immel & Lichtenthaler, 2000)

The CHAS excipients are used in the controlled release of drugs in tablets for oral administration or implants. CHAS is used in the direct compression of a large variety of drugs ranging from soluble to insoluble in water, and the release profile of the drug could be easily controlled and adapted (Ravenelle & Rahmouni, 2006). In comparison to well-known excipients such as microcrystalline cellulose or hydroxypropylmethyl cellulose, tablets made of CHAS do not dissolve or disintegrate upon hydration (Fig. 4).

3. ^{13}C NMR spectroscopy of chemically modified high amylose starch controlled drug release systems

3.1. ^{13}C NMR of starch materials

^{13}C NMR spectroscopy is widely used to assess the structure of starch samples, and to study structural changes of starch-based samples (Atichokudomchai, Varavinit, & Chinachoti, 2004; Blaszczak, Valverde, & Fornal, 2005; Deval et al., 2004). Many phenomena such as retrogradation (Baik, Dickinson, & Chinachoti, 2003; Primo-Martin, van Nieuwenhuijzen, Hamer, & van Vliet, 2007; Smits, Kruiskamp, van Soest, & Vliegenthart, 2003), gelatinization (Lin, Wang, & Chang, 2008), formation of inclusion complexes (Morgan, Furneaux, & Larsen, 1995), and enzymatic hydrolysis (Pizzoferrato, Rotilio, & Paci, 1999; Shogren et al., 1992) of the starch could be studied by ^{13}C CP/MAS NMR spectroscopy. ^{13}C NMR spectroscopy of starch is sensitive to the polymorphism of the material (Gidley & Bociek, 1985, 1988; Tan, Flanagan, Halley, Whittaker, & Gidley, 2007; Veregin, Fyfe, Marchessault, & Taylor, 1986). Amorphous and crystalline materials have different ^{13}C NMR spectra (Fig. 1). ^{13}C CP/MAS spectroscopy can be used to observe the formation, destruction, or changes of the crystalline domains following the application of different stimulus. While X-ray diffraction measures long range order, NMR spectroscopy assesses the local structure of the starch chains. The crystallinity, or order, measured by ^{13}C NMR spectroscopy is higher that the crystallinity obtained by X-ray diffraction for the same sample because only a fraction of the ordered domains probed by NMR are large enough to diffract X-rays (Barsby et al., 2001; Gidley & Bociek, 1985; Shi et al., 1998).

3.2. ^{13}C NMR of CHAS tablets

The limited swelling and the shape retention of the CHAS tablets which lead to the sustained release property are due to the retrogradation of the starch chains. The structural reorganization of

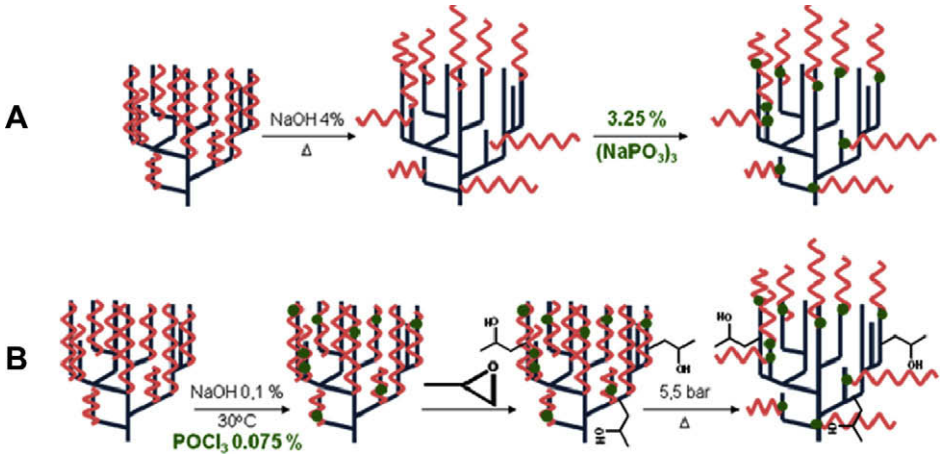

Fig. 3. Preparation methods of crosslinked high amylose starche (CHAS). (A) CHAS I (Dumoulin et al., 1998b) is prepared by the gelatinization of the starch, followed by crosslinking with 3.25% of sodium trimethaphosphate; (B) CHAS II is prepared (Lenaerts et al., 2003) by crosslinking the starch with 0.075% of phosphorus oxychloride, then functionalized with propylene oxide and followed by gelatinization. (■) Amylopectine; (■) amylose; (■) crosslinker.

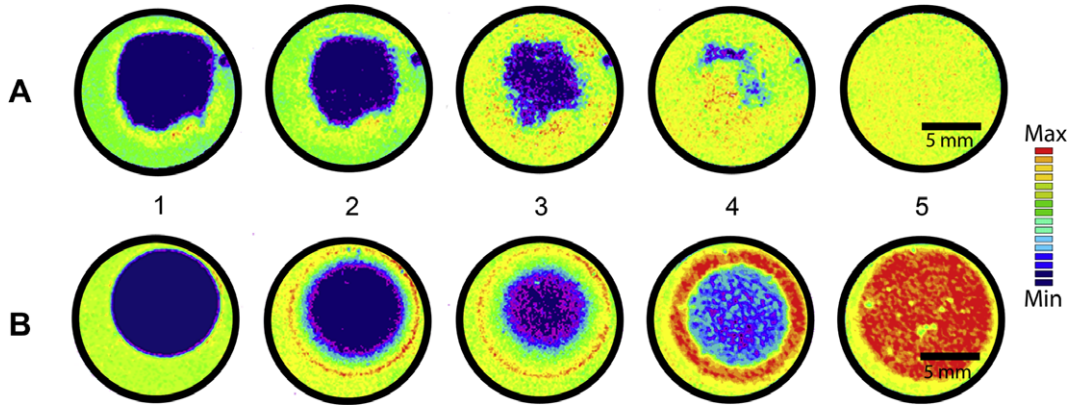

Fig. 4. NMR ^{1}H intensity images of (A) microcrystalline cellulose/mannitol tablet and (B) crosslinked high amylose starch tablet (CHAS I) during water absorption at 25 °C at different immersion times. 256 × 256 pixel images obtained with a multi-echo pulsed sequence (echo time 4 ms; repetition time 2 s; in-plane resolution 59 μm) on a spectrometer operating at 300.13 MHz. (A.1) 35 min; (A.2) 3 h; (A.3) 4 h; (A.4) 10 h; (A.5) 11 h; (B.1) 35 min; (B.2) 10 h; (B.3) 20 h; (B.4) 50 h; (B.5) 70 h.

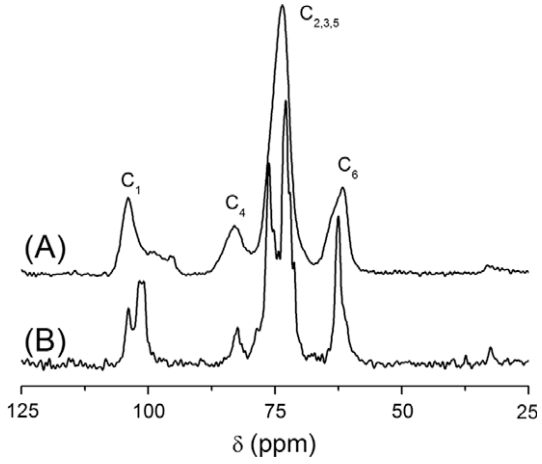

Fig. 5. ^{13}C CP/MAS NMR spectra of CHAS I obtained at 150.90 MHz with a contact time of 1.5 ms. (A) Dry CHAS; (B) Hydrated CHAS.

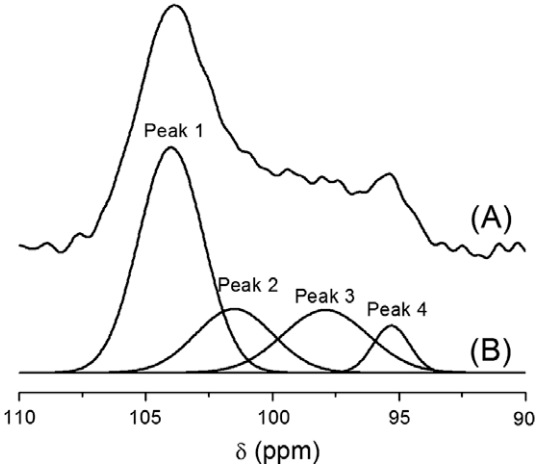

Fig. 6. ^{13}C NMR CP/MAS spectrum of dry CHAS II acquired at contact time of 1.5 ms. (A) Experimental spectrum. (B) Decomposed spectrum. Peak 1 is associated to the amorphous domains and the V-type helices. Peak 2 is characteristic of B-type helices, Peak 3 of glucose units in amorphous amylopectin, and Peak 4 of constrained linkage in an unfavored conformation produced upon spray-drying of the CHAS powder.

the starch chains can be studied by ^{13}C CP/MAS NMR spectroscopy. In the dry tablets, modified starch is mainly present as amorphous and V-type structures (Dumoulin, Alex, Szabo, Cartilier, & Mateescu, 1998a; Le Bail, Morin, & Marchessault, 1999; Shiftan, Ravenelle, Mateescu, & Marchessault, 2000). Upon hydration of starch, the amorphous domains are partially converted to B-type crystalline structures (Fig. 5) (Shiftan et al., 2000; Therien-Aubin, Janvier, Baille, Zhu, & Marchessault, 2007a). The B-type double helices act as new crosslinking points which limit the swelling and contribute to the shape retention by the formation of a tridimensional network in the whole tablet.

The ^{13}C CP/MAS NMR experiments with variable contact time presented in Figs. 5 and 6 were recorded at room temperature on a Bruker AV-600 spectrometer operating at 150.90 MHz. The samples were spun at 8 kHz, and 1000–1800 scans were accumulated. The contact time varied from 0.01 to 11 ms (Therien-Aubin et al., 2007a).

The initial dry CHAS is mainly amorphous with traces of V-type crystalline structures (Therien-Aubin et al., 2007a). Upon hydration, the narrowing and the splitting of the peaks are observed (Fig. 5), and spectral features typical of the B-type helices, such as the doublet at 100 ppm, can be observed. Le Bail et al. have shown that in highly crosslinked samples, the formation of B-type helices is not observed, the crosslinking of the starch hindering the development of double helices (Le Bail et al., 1999).

Shiftan et al. showed that the B and V polymorphs have a different sensitivity to the crosslinking density (Shiftan et al., 2000). The crosslinking density limits the capacity to form the two polymorphs, as observed by lower and broader peaks for the NMR peaks typical of the crystalline domains of B and V polymorphs. However, this effect is more pronounced for the B double helix polymorph. The formation of B-type domains needs the cooperative movements of the starch chains to form the double helices. Crosslinking points highly limit these movements. High crosslinking density even prevents the formation of the V-type single helices. The limited formation of B-type domains upon hydration is responsible of the loss of cohesion, capping and disintegration observed for tablets made of highly crosslinked CHAS.

The starch polymorphs have different NMR spectra, the region of the C1 resonance is particularly well suited to study the polymorphism of the starch samples (Bogracheva, Wang, & Hedlery, 2001; Gidley & Bociek, 1985, 1988; Paris, Bizot, Emery, Buzare, & Buleon, 2001; Paris, Bizot, Emery, Buzaré, & Buléon, 1999; Shiftan et al., 2000; Veregin et al., 1986). The spectral decomposition of this region, along with variable contact time CP/MAS experiments, allows the quantitative determination of each polymorphs in the

starch samples (Therien-Aubin et al., 2007a). Fig. 6 shows typical spectral decomposition of an NMR spectrum of dry CHAS.

^{13}C CP/MAS spectroscopy was used to compare CHAS I and CHAS II. The results obtained (Therien-Aubin et al., 2007a) shows that dry CHAS I and II contained c.a. 20% of starch organized in B-type structure, while the hydrated CHAS contained, in both cases, c.a. 60% of B-type helices. The higher degree of crosslinking of CHAS I does not limit the reorganization of the starch chains in B-type helices (Therien-Aubin et al., 2007a). The differences between the two preparation methods arise in the content of interfacial material between the B-type domains and the V-type and amorphous domains. Hydrated CHAS I contained less interfacial material between the double helices domains and the amorphous/single helix domains than the hydrated CHAS II. Therefore, the domains composed of B-type double helices are more homogeneously dispersed in hydrated CHAS II (Therien-Aubin et al., 2007a). The difference in the efficiency of the membrane at water/tablet interface, responsible of the limited swelling and sustained diffusion, is not attributed to the higher degree of crosslinking, but to the preparation method and the homogeneity of the gel membrane formed at the interface. The gelatinization of the CHAS I, prior to crosslinking, allows the segregation of the amylose and the amylopectin. Therefore, CHAS I has a more heterogeneous structure than CHAS II.

4. NMR imaging of chemically modified high amylose starch controlled drug release systems

Among the imaging techniques, NMR is appealing in the study of pharmaceutical excipients (Baumgartner, Lahajnar, Sepe, & Kristl, 2005; Fyfe & Blazek-Welsh, 2000; Kowalczuk, Tritt-Goc, & Pislewski, 2004; Rajabi-Siahboomi et al., 1994) because of its non-invasive and non-destructive nature which allows the study of the interior of any non-ferromagnetic object without physical slicing. NMR imaging can provide detailed images in any directions of the interior of an analyzed object. The contrast of NMR images typically represents the spin density of mobile protons of the system. In the study of solvent uptake, only the molecules of solvent contribute to the signal. However, contrast of the image could be adjusted by any factors measurable by NMR, such as changes in concentration (Baille, Malveau, Zhu, & Marchessault, 2002; Chowdhury, Hill, & Whittaker, 2004a; Chowdhury, Hill, Whittaker, Braden, & Patel, 2004b; Fyfe & Blazek, 1997; Malveau, Baille, Zhu, & Marchessault, 2002; Thérien-Aubin, Baille, Zhu, & Marchessault, 2005; Thérien-Aubin & Zhu, 2006; Thérien-Aubin, Zhu, Ravenelle, & Marchessault, 2008), relaxation times (Chowdhury et al., 2004b; Fyfe & Blazek, 1997; Rajabi-Siahboomi, Bowtell, Mansfield, Davies, & Melia, 1996), or self-diffusion coefficients (Bowtell et al., 1994; Kojima & Nakagami, 2002; Rajabi-Siahboomi et al., 1996; Thérien-Aubin et al., 2008; Tritt-Goc, Kowalczuk, & Pislewski, 2003). NMR imaging is widely used to follow water uptake and moisture diffusion and to assess the water distribution in a system in different polymeric and starch-based systems (Hopkinson, Jones, Black, Lane, & McDonald, 1997; Horigane, Takahashi, Maruyama, Ohtsubo, & Yoshida, 2006b; Horigane et al., 2006a; Kasai, Lewis, Ayabe, Hatae, & Fyfe, 2007; Russo et al., 2007; Ziegler, MacMillan, & Balcom, 2003). NMR imaging of pharmaceutical tablets could be used to follow the effects of solvent uptake in a single tablet at different immersion times.

Table 1
Physical characteristics of the CHAS tablets

CHAS	Drug loading	Weight (mg)	Diameter (mm)	Thickness (mm)	Compression force (kN)	Hardness (N)
I	–	200	8.5	2.6	13	198
II	–	209	8.9	3.0	22	138
II	10% Acetaminophen	205	8.7	3.0	8	145
II	10% Ciprofloxacin	202	8.6	2.8	8	130

4.1. Acquisition of NMR images of CHAS tablets

The NMR imaging experiments in the study of the drug loading effect were performed on a Bruker Avance-400 NMR spectrometer operating at 400.26 MHz for protons on different CHAS tablets (Table 1). The system was equipped with three orthogonal field gradient coils (maximum gradient of 100 G/cm). A standard spin–echo pulse sequence was used to obtain spin density images of the tablets. A slice of 0.5 mm in thickness was selected either perpendicular or parallel to the main magnetic field (axial axis) using a sinc-shaped pulse. Eight scans were accumulated to obtain 128 × 128 pixel images for a field of view of 1.5 cm, leading to an in-plane resolution of 117 μm. An echo time (TE) of 3 ms and a repetition time (TR) of 1 s were fixed leading to an acquisition time of about 17 min for each image. Self-diffusion coefficient imaging was performed under the same condition by applying a pulsed-gradient spin–echo (PGSE) sequence in the imaging pulsed sequence. In this case, the echo time, which is equal to the diffusion time (Δ), was set to 10 ms in order to achieve enough attenuation of the signal in the self-diffusion experiment. The length of the gradient pulse (δ) used in the PGSE sequence was 2 ms, and the gradient strength varied from 5 to 100 G/cm (Thérien-Aubin et al., 2008). For the study of the temperature effect, the experiments were carried on a Bruker DSX300 NMR spectrometer operating at 300.13 MHz, also equipped with similar orthogonal field gradient coils on CHAS I and CHAS II tablets (Table 1) without drug molecules. A slice 1 mm in thickness was selected either perpendicular or parallel to the main magnetic field (axial axis) using a sinc-shaped pulse. Four scans were accumulated to obtain 128 × 128 pixel images for a field of view of 2 cm, leading to an in-plane resolution of 156 μm. An echo time (TE) of 6 ms and a repetition time (TR) of 1 s were fixed leading to an acquisition time of about 8.5 min for each image (Thérien-Aubin et al., 2005). The reported errors in Tables 2–4 are standard deviation measured on triplicates.

4.2. Swelling of CHAS tablets

Upon immersion of a tablet in water, both the water uptake and the swelling of the tablet can be observed by NMR imaging. The swelling of the tablet, shown by its variation in size, is characterized by the percentage of swelling (S)

$$S(t) = \frac{d(t) - d_0}{d_0} \times 100 \quad (1)$$

where $d(t)$ is the dimension of the tablet at an immersion time t, and d_0 the initial dimension of the tablet. Fig. 7 shows typical swelling kinetics of CHAS tablets. The swelling rates (k_s) are obtained from the fits of

$$S(t) = S_{\max}(1 - e^{-k,t}) + S_0 \quad (2)$$

where $S_{\max}$ is the maximal swelling observed at the equilibrium and S_0 the swelling caused by the sorption of moisture present in the air.

The swelling observed upon immersion of the tablet in water is limited and anisotropic (Malveau et al., 2002; Thérien-Aubin & Zhu, 2006; Thérien-Aubin et al., 2005, 2008). The limited swelling, leading to the shape retention of the tablet and the prevention of tablet dissolution or erosion, is caused by the reorganization of the hydrated starch chains (Le Bail et al., 1999; Ravenelle & Rahmouni, 2006). The reorganization of the starch chains was evidenced by ^{13}C NMR spectroscopy as discussed in the precedent

Table 2
Swelling characteristics of the CHAS II tablets in water

Drug loading	Temperature (°C)	Radial swelling		Axial swelling	
		S_{max} (%)	k (10^{-3} min^{-1})	S_{max} (%)	k (10^{-3} min^{-1})
–	25	22 ± 2	3 ± 1	44 ± 5	8 ± 3
–	37	23 ± 2	6 ± 3	55 ± 3	8 ± 2
–	45	20 ± 5	8 ± 2	56 ± 3	30 ± 7
–	60	72 ± 3	12 ± 5	103 ± 5	59 ± 6
10% Acetaminophen	37	27 ± 3	5 ± 1	62 ± 6	7 ± 3
10% Ciprofloxacin	37	24 ± 2	6 ± 1	54 ± 3	8 ± 2
10% Ciprofloxacin[a]	37	22 ± 2	7 ± 1	52 ± 4	8 ± 2

[a] Experiments performed in an aqueous solution of ciprofloxacin (0.03 g/mL).

Table 3
Characteristics of water uptake in the CHAS II tablets

Drug loading	Temperature (°C)	NMR integration		Profile fit
		$\bar{D}$ (10^{-11} m^2/s)	n	D (10^{-11} m^2/s)
–	25	1.1 ± 0.1	0.4 ± 0.1	3.9 ± 0.6
–	37	2.0 ± 0.3	0.5 ± 0.1	6.3 ± 0.4
–	45	2.60 ± 0.03	0.51 ± 0.04	8 ± 1
–	60	–	0.9 ± 0.1	16 ± 1
10% Acetaminophen	37	3.9 ± 0.2	0.54 ± 0.06	7.2 ± 0.5
10% Ciprofloxacin	37	6.1 ± 0.5	0.49 ± 0.07	8.1 ± 0.6
10% Ciprofloxacin[a]	37	5.3 ± 0.4	0.44 ± 0.06	7.3 ± 0.8

$\bar{D}$, average diffusion coefficient calculated with Eq. (4) from fits of Eq. (3) to the experimental data.
n, water uptake kinetic parameter, obtained from fits of Eq. (3).
D, diffusion coefficient measured from fits of Eq. (5).
[a] Experiments performed in an aqueous solution of ciprofloxacin (0.03 g/mL).

Table 4
Comparison of tablets made of CHAS I and CHAS II

CHAS	Temperature (°C)	Swelling		Water uptake
		Radial (%)	Axial (%)	$\bar{D}$ (10^{-11} m^2/s)
I	25	24 ± 3	–	1.9 ± 0.1
I	37	38 ± 3	76 ± 5	2.7 ± 0.1
II	25	22 ± 2	44 ± 5	1.1 ± 0.1
II	37	23 ± 2	55 ± 3	2.0 ± 0.3

section. Table 2 shows the anisotropic swelling of the CHAS tablet evidenced by a larger swelling in thickness (axial) than in diameter (radial) (Malveau et al., 2002; Thérien-Aubin et al., 2005). The phenomenon is related to the preparation process of the tablets. During the tablet compression, the force is applied in the axial direction, the thickness, and the spherical starch particles are compressed into irregular disk. Upon immersion in water and tablet hydration, the stress is released and the particles regain their original shape, leading to a larger swelling in the direction of the applied compression force (Le Bail et al., 1999).

4.3. Water uptake and diffusion coefficient

NMR imaging can be used to monitor directly the penetration of water in the tablet. The solvent penetration is commonly measured by gravimetric method. However, gravimetric studies of CHAS tablets do not lead to quantitatively interpretable data due to the abrasion of the tablets (Malveau et al., 2002; Thérien-Aubin et al., 2005). NMR imaging studies can bypass this problem and allow the measurement of the average diffusion coefficient of water in unperturbed systems as the gravimetric studies and also the

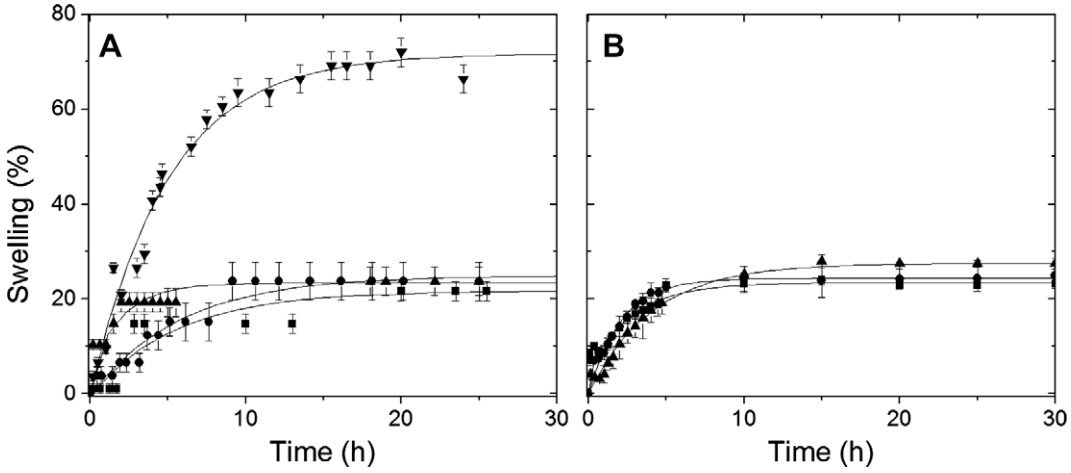

Fig. 7. Radial swelling kinetics of the CHAS II tablets. (A) Temperature effect; (■) 25 °C, (●) 37 °C, (▲) 45 °C, and (▼) 60 °C. (B) Drug loading effect; (■) no drug, (●) acetaminophen (10 wt.%), and (▲) ciprofloxacin (10 wt.%). Fits to Eq. (2) are shown.

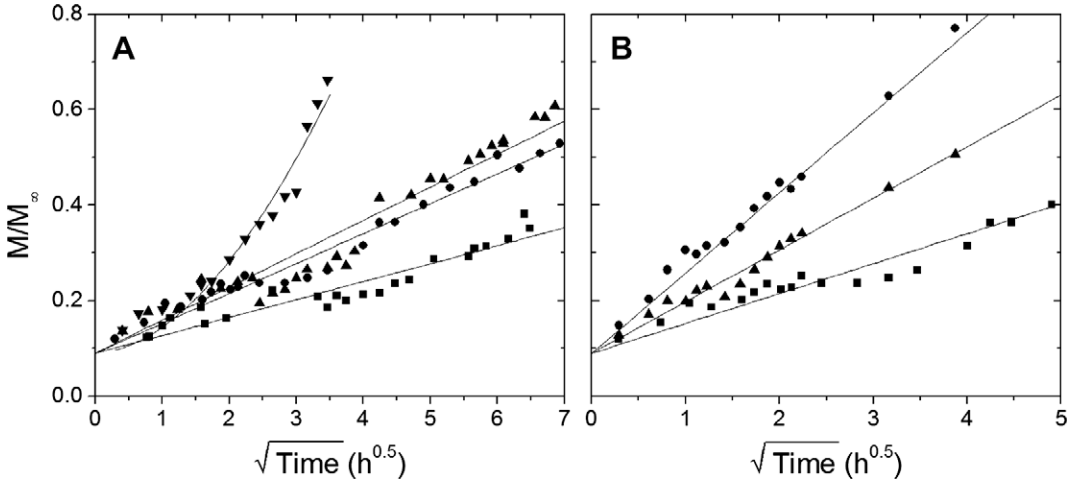

Fig. 8. Water penetration (relative weight gain) kinetics in CHAS II tablets as observed by NMR. (A) Temperature effect; (■) 25 °C, (●) 37 °C, (▲) 45 °C, and (▼) 60 °C. (B) Drug loading effect; (■) no drug, (●) acetaminophen (10 wt.%), and (▲) ciprofloxacin (10 wt.%). Fits to Eq. (3) are shown.

'instantaneous' diffusion coefficient (Thérien-Aubin et al., 2005, 2008). Furthermore, NMR imaging with contrast resolved by self-diffusion coefficient can be used to follow the mobility of the water molecules according to their location in the tablet (Thérien-Aubin et al., 2008).

The average diffusion coefficient is measured from the pseudo-gravimetric measurements (Fig. 8), which can be described by (Alfrey, Gurnee, & Lloyd, 1966)

$$\frac{M_t}{M_\infty} = \frac{\int C_t dx}{\int C_\infty dx} = k_d t^n + M_0 \quad (3)$$

where M_t is the amount of water having diffused after an immersion time t, M_0 the amount of water present in the polymer matrix before the immersion in the solvent, M_∞ the amount of water in the polymer matrix at the equilibrium, and k_d a parameter related to the velocity or to the diffusion coefficient of the water uptake. M_t is proportional to integration of the NMR image intensity (the water concentration) over space. The parameter n describes the kinetics of the water uptake and is equal to 0.5 for Fickian diffusion and to 1 for Case II diffusion. Intermediate values of n indicate an anomalous diffusion process. If the diffusion is Fickian, the average diffusion coefficient ($\bar{D}$) in a cylindrical polymer sample of radius r is given by (Crank & Park, 1968)

$$\bar{D} = \left(\frac{k_d \pi r}{4}\right)^2 \quad (4)$$

When the diffusion process is Fickian, the 'instantaneous' diffusion coefficient can be measured by fittings of the second Fick's law of diffusion to the water concentration profiles obtained by NMR imaging (Fig. 9). Fick's law relates the diffusion coefficient to the concentration gradient of the diffusing species. This concentration (C) in an infinitely long cylinder of radius r after an immersion time t is then described by (Crank, 1979)

$$\frac{C - C_0}{C_\infty - C_0} = 1 - \frac{2}{r}\sum_{n=1}^{\infty} \frac{J_0(x\alpha_n)}{\alpha_n J_1(r\alpha_n)} e^{-D\alpha_n^2 t} \quad (5)$$

where x is a given position inside the tablet, C_0 the initial concentration of the diffusive species in the tablet, C_∞ the concentration of the diffusive species once equilibrium is obtained, and J_n the Bessel function of the first kind of order n and α_n the nth root of J_0.

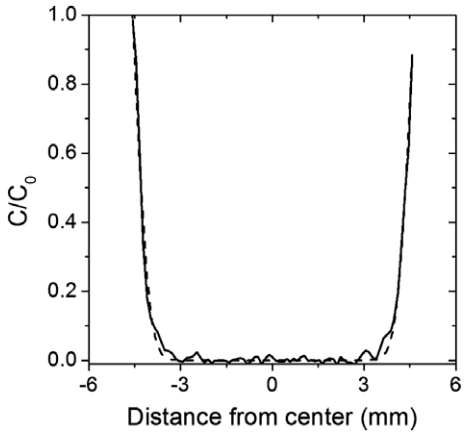

Fig. 9. Water concentration profile in a CHAS II tablet loaded with 10 wt.% acetaminophen after 30 min of immersion in water at 37 °C. Solid line, experimental results; dashes, fits to Eq. (5).

The results presented in Table 3 show that the average diffusion coefficient (calculated with Eq. (4) from fits of Eq. (3) to the relative NMR water uptake measurements) is lower than the 'instantaneous' diffusion coefficient measured after 30 min of hydration from fits of Eq. (5) to the water profile obtained by NMR imaging (Thérien-Aubin et al., 2005, 2008). This is caused by the formation of a gel membrane at the water/tablet interface. This membrane, evidenced by NMR imaging (Baille et al., 2002; Malveau et al., 2002; Thérien-Aubin et al., 2005, 2008) as well as other imaging techniques such as electron microscopy and X-ray microtomography (Chauve, Ravenelle, & Marchessault, 2007), has a lower porosity than the core of the tablet and reduces the diffusion coefficient of water.

4.4. Temperature effect

Both swelling and water uptake are affected by the temperature of the system. Between 25 and 60 °C, the swelling rate increases with temperature. On the basis of the swelling rate, an activation energy for the swelling process of 42 ± 8 kJ/mol was calculated (Thérien-Aubin et al., 2005). However, the percentage of swelling observed for the CHAS tablet is the same between 25 and 45 °C within the experimental errors, while at 60 °C the percentage of swelling is twice of the value observed at lower temperatures. The limited swelling observed between 25 and 45 °C is ascribed to the reorganization of the starch chains in the crystalline domains (Thérien-Aubin et al., 2005). The results observed show that

the mechanical properties of the network formed upon hydration by the formation of the B-type double helices is not altered by the temperature variations. The gelatinization of a suspension of CHAS powder in water is observed between 60 and 100 °C (Ravenelle & Rahmouni, 2006). The gelatinization is associated with the loss of the crystalline domains. At 60 °C, the gelatinization disrupts the B-type double helices, which are responsible of the limited swelling observed at lower temperature, leading to the formation of a weaker network which gives rise to an increase in swelling.

Fig. 8A shows that the diffusion process is Fickian between 25 and 45 °C and Case II at 60 °C. A Fickian diffusive behavior is characterized by a linear relation between the water uptake and the squared root of the immersion time. Frisch et al. have shown for various polymer-solvent systems that for a given pair of polymer-diffusant different diffusive behaviors might be observed when temperature is varied, since both the water uptake and the relaxation rate of the polymer matrix increases when the temperature is raised (Frisch, 1980). Fickian diffusion is only observed when the relaxation of the polymer network does not interfere with the diffusion process and proceeds on a different time scale from the diffusion process. Case II diffusion, as for CHAS tablet immersed in water at 60 °C, is observed when the rate of relaxation and diffusion are similar.

In the case where the diffusion process is Fickian, Eq. (4) can be used to measure the average diffusion coefficient. The diffusion coefficient increases when the temperature is raised. The activation energy for the diffusion process (35 ± 5 kJ/mol) (Thérien-Aubin et al., 2005) is lower than the activation energy measured for the swelling process. This difference could be explained by the fact that while the diffusion process only involves movement of water molecules, swelling is the combined result of the movement of water molecules and of starch chains.

4.5. Drug loading effect

The swelling and water uptake of tablets containing drugs at 10 wt.% loading were analyzed in water at 37 °C. The two drugs studied, acetaminophen and ciprofloxacin, have different solubility and hydrodynamic radius. Ciprofloxacin is more soluble in water (3.5 g/100 mL) than acetaminophen (1.4 g/100 mL) and has a larger hydrodynamic radius (R_h 0.65 nm vs 0.37 nm). Table 2 shows that the presence of the drug does not influence the swelling of the tablets within the limits of the experimental errors; analysis of the results with *t*-test ($\alpha = 0.05$) shows that all the samples at 37 °C are statistically equivalent. The presence of the drug at a loading of 10 wt.% is insufficient to alter the mechanical properties of the 3D network formed upon hydration by the B-type double helices (Thérien-Aubin et al., 2008).

Fig. 8B shows that the average diffusion coefficients of water in the tablet increase in presence of a drug in the CHAS tablets. The higher diffusion coefficient is ascribed to the higher gradient of chemical potential at the water/tablet interface, but not to a coarser tablet structure caused by the dissolution of the drug (Thérien-Aubin et al., 2008). Fig. 10 clearly shows that the mobility (self-diffusion coefficient) of water is the same in the tablets with and without drugs, the maximal reduced self-diffusion coefficient, as observed in the membrane, is equivalent in the three types of tablets. Therefore, the structure of the hydrated CHAS is similar in the three types of tablets, since a coarser structure will have been evidenced by a higher reduced self-diffusion coefficient. Furthermore, the presence of a gradient of chemical potential at the water/tablet interface was shown by a water uptake experiment in a solution of ciprofloxacin rather than in water. In the presence of the drug in the surrounding media of the tablet, the diffusion coefficient of water in the tablet decreases (Table 3), since the presence of the dissolved drug decreases the chemical potential of the media and thus decreases the gradient of chemical potential between the media and the dry tablet (Thérien-Aubin et al., 2008).

NMR imaging could be used to correlate the drug release with the water uptake in order to get a better understanding of the drug release process. Fig. 11A shows that the release of acetaminophen is faster than the release of ciprofloxacin, even though Fig. 8B shows that water uptake in ciprofloxacin-loaded tablet is faster. This phenomenon can be ascribed to the smaller hydrodynamic radius of acetaminophen (Thérien-Aubin et al., 2008). The mobility of the dissolved acetaminophen molecule is higher that of ciprofloxacin because acetaminophen is a smaller molecule (Thérien-Aubin et al., 2008). These results are in keeping with the diffusion studies in model hydrogels which showed that, in absence of any specific interactions between the diffusant (the drug) and the network (the tablet), the size of the diffusing molecule is the main factor affecting the diffusion (Therien-Aubin, Zhu, Moorefield, Kotta, & Newkome, 2007b). Fig. 11B clearly demonstrates that, because of the higher mobility of acetaminophen, a lower hydration of the tablet is needed to achieve the same release as in the case of ciprofloxacin-loaded tablets (Thérien-Aubin et al., 2008).

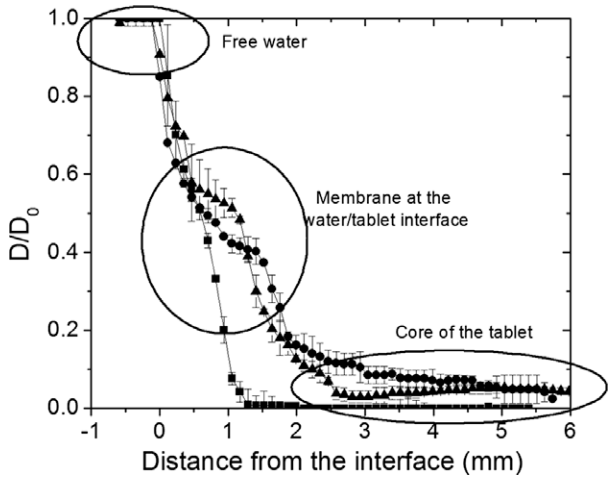

Fig. 10. Mobility (D/D_0) of water in CHAS II tablets obtained by self-diffusion coefficient NMR imaging in tablets (■) without drugs, (●) with 10 wt.% acetaminophen, and (▲) with 10 wt.% ciprofloxacin.

4.6. Effect of preparation methods

The differences between the two methods presented in Fig. 3 reside in the order of the modification steps (gelatinization and crosslinking). Even though both methods are similar, the tablets produced with the different CHAS powder, have very different behaviors (Thérien-Aubin & Zhu, 2006). Table 4 shows that the water uptake is faster in CHAS I tablets, and these tablets swell more extensively.

In a typical polymer system, a higher degree of crosslinking leads to a reduced swelling (Flory, 1953). However, in the CHAS tablets a higher degree of crosslinking leads to a higher swelling, because the crosslinks here hinder the reorganization of the starch chains in B-type double helices leading to the formation of a weaker network in the tablet (Lenaerts et al., 1998; Moussa & Cartilier, 1996). The increased swelling of CHAS tablets is followed by faster water uptake and faster drug release (Lenaerts et al., 1991).

The differences between CHAS I and II was, first, ascribed to their different degrees of crosslinking (Thérien-Aubin & Zhu, 2006). However, a detailed study of the reorganization of the starch chains by ^{13}C CP/MAS NMR, discussed in more detail previously, shows that the differences between the two types of tablets

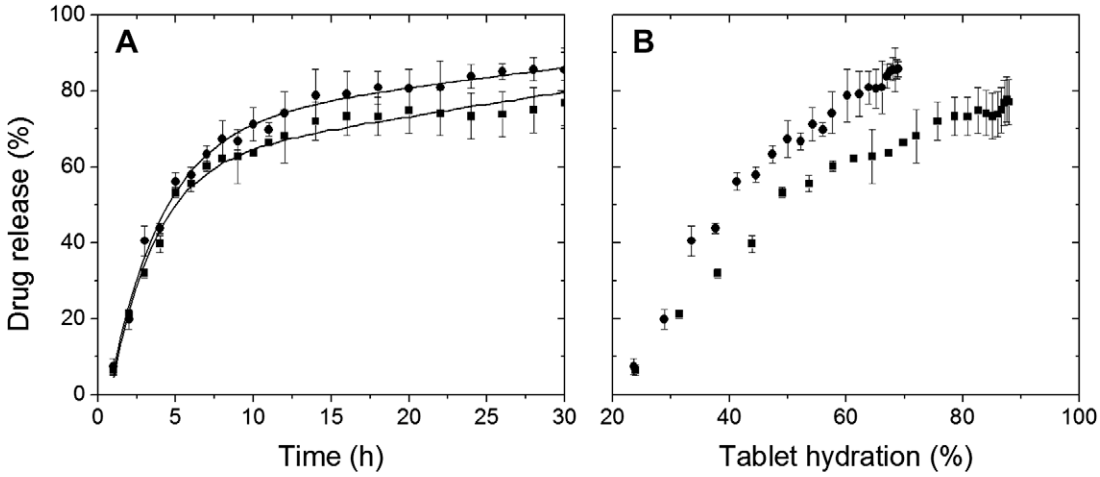

Fig. 11. (A) Kinetics of drug release from CHAS II tablets loaded with 10 wt.% (●) acetaminophen and (■) ciprofloxacin. (B) Influence of water uptake on drug release.

should be ascribed to the formation of a more heterogenous material in the case of CHAS I (Therien-Aubin et al., 2007a).

5. Conclusion

NMR techniques are valuable in the characterization of pharmaceutical excipients. Crosslinked high amylose starch is an innovative excipient, and the understanding of its behavior obtained with the NMR techniques could be used to develop new and more efficient drug release formulation. NMR imaging is a non-invasive and non-destructive technique which provides images of the interior of an object, and quantitative information on both swelling and diffusion kinetics. However, the information on the water uptake measurements itself are insufficient to explain fully the drug release kinetics observed in CHAS tablets since the physical characteristics of the drugs are also key factors. Solid state ^{13}C CP/MAS NMR spectroscopy allows the observation of structural changes in starch. The use of CP/MAS NMR with variable contact times permits the quantification of each of the starch polymorphs, allowing the analysis of the conformational changes observed upon hydration of the CHAS tablets.

Acknowledgements

The authors acknowledge the financial support from NSERC and the Canada Research Chair program.

References

Alfrey, T. J., Gurnee, E. F., & Lloyd, W. G. (1966). Diffusion in glassy polymers. *Journal of Polymer Science, Part C: Polymer Symposia, 12*, 249–261.

Atichokudomchai, N., Varavinit, S., & Chinachoti, P. (2004). A study of ordered structure in acid-modified tapioca starch by^{13} C CP/MAS solid state NMR. *Carbohydrate Polymers, 58*, 383–389.

Baik, M. Y., Dickinson, L. C., & Chinachoti, P. (2003). Solid-state^{13} C CP/MAS NMR studies on aging of starch in white bread. *Journal of Agricultural and Food Chemistry, 51*(5), 1242–1248.

Baille, W. E., Malveau, C., Zhu, X. X., & Marchessault, R. H. (2002). NMR imaging of high-amylose starch tablets. 1. Swelling and water uptake. *Biomacromolecules, 3*(1), 214–218.

Barsby, T. L., Donald, A. M., & Frazier, P. J. (2001). *Starch: Advances in structure and function*. Cambridge: The Royal Society of Chemistry.

Baumgartner, S., Lahajnar, G., Sepe, A., & Kristl, J. (2005). Quantitative evaluation of polymer concentration profile during swelling of hydrophilic matrix tablets using ^{1} H NMR and MRI methods. *European Journal of Pharmaceutics and Biopharmaceutics, 59*(2), 299–306.

Blaszczak, W., Valverde, S., & Fornal, J. (2005). Effect of high pressure on the structure of potato starch. *Carbohydrate Polymers, 59*(3), 377–383.

Bogracheva, T. Y., Morris, V. J., Ring, S. G., & Hedley, C. L. (1998). The granular structure of C-type pea starch and its role in gelatinization. *Biopolymers, 45*(4), 323–332.

Bogracheva, T. Y., Wang, Y. L., & Hedlery, C. L. (2001). The effect of water content on the ordered/disordered structures in starches. *Biopolymers, 58*, 247–259.

Bowtell, R., Sharp, J. C., Peters, A., Mansfield, P., Rajabi-Siahboomi, A. R., Davies, M. C., & Melia, C. D. (1994). NMR microscopy of hydrating hydrophilic matrix pharmaceutical tablets. *Magnetic Resonance Imaging, 12*(2), 361–364.

Buleon, A., Colonna, P., Planchot, V., & Ball, S. (1998). Starch granules: Structure and biosynthesis. *International Journal of Biological Macromolecules, 23*(2), 85–112.

Bulpin, P. V., Welsh, E. J., & Morris, E. R. (1982). Physical characterization of amylose-fatty acid complexes in starch granules and in solution. *Starch/Staerke, 34*(10), 335–339.

Cartilier, L., Ungur, M., Chebli, C. (2006). Tablet formulation for sustained drug release comprising a starch derivative matrix. International Patent Office, Pat. No. WO 2006/066399.

Case, S. E., Capitani, T., Whaley, J. K., Shi, Y. C., Trzasko, P., Jeffcoat, R., et al. (1998). Physical properties and gelation behavior of a low-amylopectin maize starch and other high-amylose maize starches. *Journal of Cereal Science, 27*(3), 301–314.

Chauve, G., Ravenelle, F., & Marchessault, R. H. (2007). Comparative imaging of a slow-release starch excipient tablet: Evidence of membrane formation. *Carbohydrate Polymers, 70*(8), 61–67.

Chebli, C., Moussa, I., Buczkowski, S., & Cartilier, L. (1999). Substituted amylose as a matrix for sustained drug release. *Pharmaceutical Research, 16*(9), 1436–1440.

Chowdhury, M. A., Hill, D. J. T., & Whittaker, A. K. (2004a). NMR imaging of the diffusion of water at 37 °C into poly(2-hydroxyethyl methacrylate) containing aspirin or vitamin B_{12}. *Biomacromolecules, 5*(3), 971–976.

Chowdhury, M. A., Hill, D. J. T., Whittaker, A. K., Braden, M., & Patel, M. P. (2004b). NMR imaging of the diffusion of water at 310 K into semi-IPNs of PEM and poly(HEMA-co-THFMA) with and without chlorhexidine diacetate. *Biomacromolecules, 5*(4), 1405–1411.

Crank, J. (1979). *The mathematics of diffusion*. Oxford: Clarendon Press.

Crank, J., & Park, G. S. (1968). *Diffusion in polymers*. London: Academic Press.

Deval, F., Crini, G., Bertini, S., Morin-Crini, N., Badot, P. M., Verbrel, J., et al. (2004). Characteization of crosslinked starch materials with spectrocopic techniques. *Journal of Applied Polymer Science, 93*, 2650–2663.

Dumoulin, Y., Alex, S., Szabo, P., Cartilier, L., & Mateescu, M. A. (1998a). Crosslinked amylose as matrix for drug controlled release. X-Ray and FT-IR structural analysis. *Carbohydrate Polymers, 37*(4), 361–370.

Dumoulin, Y., Carriere, F., Ingenito, A. (1998b). Industrial manufacture of crosslinked amylose in aqueous media, useful as an slow-release excipient. International Patent Office, Pat. No. WO 98/35992.

Flory, P. J. (1953). *Principles of polymer chemistry*. Ithaca: Cornell University Press.

Frisch, H. L. (1980). Sorption and transport in glassy-polymers. *Polymer Engineering and Science, 20*(1), 2–13.

Fyfe, C. A., & Blazek-Welsh, A. I. (2000). Quantitative NMR imaging study of the mechanism of drug release from swelling hydroxypropyl Me cellulose tablets. *Journal of Controlled Release, 68*(3), 313–333.

Fyfe, C. A., & Blazek, A. I. (1997). Investigation of hydrogel formation from hydroxypropylmethylcellulose (HPMC) by NMR spectroscopy and NMR imaging techniques. *Macromolecules, 30*(20), 6230–6237.

Gidley, M. J. (1989). Molecular mechanisms underlying amylose aggregation and gelation. *Macromolecules, 22*(1), 351–358.

Gidley, M. J., & Bociek, S. M. (1985). Molecular organization in starches: A^{13} C CP/MAS NMR study. *Journal of the American Chemical Society, 107*, 7040–7044.

Gidley, M. J., & Bociek, S. M. (1988). ^{13} C CP/MAS NMR studies of amylose inclusion complexes, cyclodextrins, and the amorphous phase of starch granules: Relationships between glycosidic linkage conformation and solid-state^{13} C chemical shifts. *Journal of the American Chemical Society, 110*(12), 3820–3829.

Hopkinson, I., Jones, R. A. L., Black, S., Lane, D. M., & McDonald, P. J. (1997). Fickian and case II diffusion of water into amylose: A stray field NMR study. *Carbohydrate Polymers, 34*(1–2), 39–47.

Horigane, A. K., Naito, S., Kurimoto, M., Irie, K., Yamada, M., Motoi, H., et al. (2006a). Moisture distribution and diffusion in cooked spaghetti studied by NMR imaging and diffusion model. *Cereal Chemistry, 83*(3), 235–242.

Horigane, A. K., Takahashi, H., Maruyama, S., Ohtsubo, K., & Yoshida, M. (2006b). Water penetration into rice grains during soaking observed by gradient echo magnetic resonance imaging. *Journal of Cereal Science, 44*(3), 307–316.

Imberty, A., Buleon, A., Vinh, T., & Perez, S. (1991). Recent advances in knowledge of starch structure. *Starch/Staerke, 43*(10), 375–384.

Imberty, A., Chanzy, H., Perez, S., Buleon, A., & Tran, V. (1988). The double-helical nature of the crystalline part of A-starch. *Journal of Molecular Biology, 201*(2), 365–378.

Immel, S., & Lichtenthaler, F. W. (2000). The hydrophobic topographies of amylose and its blue iodine complex. *Starch/Staerke, 52*(1), 1–8.

Joensson, M., Gustavsson, N.O., Laakso, T., Reslow, M. (2002). Biodegradable controlled release microparticles containing amylopectin-based starch of reduced molecular weight. International Patent Office, Pat. No. WO 2002/028370.

Kasai, M., Lewis, A. R., Ayabe, S., Hatae, K., & Fyfe, C. A. (2007). Quantitative NMR imaging study of the cooking of japonica and indica rice. *Food Research International, 40*(8), 1020–1029.

Kojima, M., & Nakagami, H. (2002). Investigation of water mobility and diffusivity in hydrating micronized low-substituted hydroxypropyl cellulose, hydroxypropylmethyl cellulose, and hydroxypropyl cellulose matrix tablets by magnetic resonance imaging (MRI). *Chemical & Pharmaceutical Bulletin, 50*(12), 1621–1624.

Kowalczuk, J., Tritt-Goc, J., & Pislewski, N. (2004). The swelling properties of hydroxypropyl methyl cellulose loaded with tetracycline hydrochloride: Magnetic resonance imaging study. *Solid State Nuclear Magnetic Resonance, 25*(1–3), 35–41.

Le Bail, P., Morin, F. G., & Marchessault, R. H. (1999). Characterization of a crosslinked high amylose starch excipient. *International Journal of Biological Macromolecules, 26*, 193–200.

Lefevre, P., Fuertes, P., Quettier, C. (2001). Excipients and disintegrants based on starch and their manufacture. European Patent Office, Pat. No. EP 1106646.

Lenaerts, V., Beck, R. H. F., Van Bogaert, E., Chouinard, F., Hopcke, R., & Desevaux, C. (2003). Crosslinked high amylose starch having functional groups as a matrix for the slow release of pharmaceutical agents. US Patent Office, Pat. No. US 6,607,748.

Lenaerts, V., Chouinard, F., Mateescu, M. A., & Ispas-Szabo, P. (2002). Crosslinked high amylose starch having functional groups as a matrix for the slow release of pharmaceutical agents. US Patent Office, Pat. No. US 6,419,957.

Lenaerts, V., Dumoulin, Y., & Mateescu, M. A. (1991). Controlled release of theophylline from crosslinked amylose tablets. *Journal of Controlled Release, 15*(1), 39–46.

Lenaerts, V., Moussa, I., Dumoulin, Y., Mebsout, F., Chouinard, F., Szabo, P., et al. (1998). Crosslinked high amylose starch for controlled release of drugs: Recent advances. *Journal of Controlled Release, 53*(1–3), 225–234.

Lin, J. H., Wang, S. W., & Chang, Y. H. (2008). Effect of molecular size on gelatinization thermal properties before and after annealing of rice starch with different amylose contents. *Food Hydrocolloids, 22*(1), 156–163.

Malveau, C., Baille, W. E., Zhu, X. X., & Marchessault, R. H. (2002). NMR imaging of high-amylose starch tablets. 2. Effect of tablet size. *Biomacromolecules, 3*(6), 1249–1254.

Mateescu, M. A., Lenaerts, V., & Dumoulin, Y. (1992). Use of crosslinked amylose as a matrix for slow-release oral pharmaceutical compositions. US Patent Office, Pat. No. US 5,456,921.

Miles, M. J., Morris, V. J., Orford, P. D., & Ring, S. G. (1985). The roles of amylose and amylopectin in the gelation and retrogradation of starch. *Carbohydrate Research, 135*(2), 271–281.

Morgan, K. R., Furneaux, R. H., & Larsen, N. G. (1995). Solid-state NMR studies on the structures of starch granules. *Carbohydrate Research, 276*, 387–399.

Morgan, K. R., Furneaux, R. H., & Stanley, R. A. (1992). Observation by solid-state ^{13} C CP/MAS NMR spectroscopy of the transformations of wheat starch associated with the making and staling of bread. *Carbohydrate Research, 235*, 15–22.

Morrison, W. R., Tester, R. F., & Gidley, M. J. (1994). Properties of damaged starch granules. II. Crystallinity, molecular order and gelatinization of ball-milled starches. *Journal of Cereal Science, 19*(3), 209–217.

Moussa, I. S., & Cartilier, L. H. (1996). Characterization of moving fronts in crosslinked amylose matrixes by image analysis. *Journal of Controlled Release, 42*(1), 47–55.

O'Neil, M. J. (2006). *The Merck index: An encyclopedia of chemicals, drugs, and biologicals*. Whitehouse Station, NJ: Merck & Co.

Paris, M., Bizot, H., Emery, J., Buzare, J. Y., & Buleon, A. (2001). NMR local range investigations in amorphous starchy substrates I. Structural heterogeneity probed by^{13} C CP/MAS NMR. *International Journal of Biological Macromolecules, 29*(2), 127–136.

Paris, M., Bizot, H., Emery, J., Buzaré, J. Y., & Buléon, A. (1999). Crystallinity and structuring role of water in native and recrystallized starches by^{13} C CP/MAS NMR spectroscopy 1: Spectral decomposition. *Carbohydrate Polymers, 39*, 327–339.

Pizzoferrato, L., Rotilio, G., & Paci, M. (1999). Modification of structure and digestibility of chestnut starch upon cooking: A solid state^{13} C CP MAS NMR and enzymatic degradation study. *Journal of Agricultural and Food Chemistry, 47*(10), 4060–4063.

Pope, D. G., & Royce, A. E. (1987). Multilayer drug delivery device with alternate layers of drug in swellable material and spacers, for intermittent delivery of drugs. European Patent Office, Pat. No. EP 246819.

Primo-Martin, C., van Nieuwenhuijzen, N. H., Hamer, R. J., & van Vliet, T. (2007). Crystallinity changes in wheat starch during the bread-making process: Starch crystallinity in the bread crust. *Journal of Cereal Science, 45*(2), 219–226.

Rajabi-Siahboomi, A. R., Bowtell, R. W., Mansfield, P., Davies, M. C., & Melia, C. D. (1996). Structure and behavior in hydrophilic matrix sustained release dosage forms: 4. Studies of water mobility and diffusion coefficients in the gel layer of HPMC tablets using NMR imaging. *Pharmaceutical Research, 13*(3), 376–380.

Rajabi-Siahboomi, A. R., Bowtell, R. W., Mansfield, P., Henderson, A., Davies, M. C., & Melia, C. D. (1994). Structure and behavior in hydrophilic matrix sustained-release dosage forms: 2. NMR-imaging studies of dimensional changes in the gel layer and core of HPMC tablets undergoing hydration. *Journal of Controlled Release, 31*(2), 121–128.

Ravenelle, F., & Rahmouni, M. (2006). Contramid: High-amylose starch for controlled drug delivery. In R. H. Marchessault, F. Ravenelle, & X. X. Zhu (Eds.), *Polysaccharides for Drug Delivery and Pharmaceutical Applications* (pp. 79–104). New York: ACS Symposium Series.

Robyt, J. F. (1998). *Essentials of Carbohydrate Chemistry*. New York: Springer.

Rowe, R. C., Sheskey, P. J., & Weller, P. J. (2003). *Handbook of pharmaceutical excipients*. London: Pharmaceutical Press.

Rudnic, E. M., McCarty, J. A., & Belenduik, G. W. (1996). Sustained-release drug delivery system comprising a highly soluble pharmaceuticals. US Patent Office, Pat. No. US 5,484,608.

Russo, M. A. L., Strounina, E., Waret, M., Nicholson, T., Truss, R., & Halley, P. J. (2007). A study of water diffusion into a high-amylose starch blend: The effect of moisture content and temperature. *Biomacromolecules, 8*(1), 296–301.

Shi, Y.-C., Capitani, T., Trzasko, P., & Jeffcoat, R. (1998). Molecular structure of a low-amylopectin starch and other high-amylose maize starches. *Journal of Cereal Science, 27*(3), 289–299.

Shiftan, D., Ravenelle, F., Mateescu, M. A., & Marchessault, R. H. (2000). Change in the V/B polymorph ratio and T_1 relaxation of epichlorohydrin crosslinked high amylose starch excipient. *Starch/Staerke, 52*(6–7), 186–195.

Shogren, R. L., Thompson, A. R., Felker, F. C., Harryokuru, R. E., Gordon, S. H., Greene, R. V., et al. (1992). Polymer compatibility and biodegradation of starch poly(ethylene-co-acrylic acid) polyethylene blends. *Journal of Applied Polymer Science, 44*(11), 1971–1978.

Smits, A. L. M., Kruiskamp, P. H., van Soest, J. J. G., & Vliegenthart, J. F. G. (2003). The influence of various small plasticisers and malto-oligosaccharides on the retrogradation of (partly) gelatinised starch. *Carbohydrate Polymers, 51*(4), 417–424.

Tan, I., Flanagan, B. M., Halley, P. J., Whittaker, A. K., & Gidley, M. J. (2007). A method for estimating the nature and relative proportions of amorphous, single, and double-helical components in starch granules by^{13} C CP/MAS NMR. *Biomacromolecules, 8*(3), 885–891.

Te Wierik, G. H. P., Eissens, A. C., Bergsma, J., Arends-Scholte, A. W., & Lerk, C. F. (1997). A new generation of starch products as excipient in pharmaceutical tablets. II. High surface area retrograded pregelatinized potato starch products in sustained-release tablets. *Journal of Controlled Release, 45*(1), 25–33.

Thérien-Aubin, H., Baille, W. E., Zhu, X. X., & Marchessault, R. H. (2005). Imaging of high-amylose starch tablets. 3. Initial diffusion and temperature effect. *Biomacromolecules, 6*, 3367–3372.

Therien-Aubin, H., Janvier, F., Baille, W. E., Zhu, X. X., & Marchessault, R. H. (2007a). Study of hydration of cross-linked high amylose starch by solid state^{13} C NMR spectroscopy. *Carbohydrate Research, 342*(11), 1525–1529.

Thérien-Aubin, H., & Zhu, X. X. (2006). Water diffusion in drug delivery systems made of high-amylose starch as studied by NMR imaging. In R. H. Marchessault, F. Ravenelle, & X. X. Zhu (Eds.), *Polysaccharides for drug delivery and pharmaceutical applications* (pp. 105–120). New York: ACS Symposium Series.

Therien-Aubin, H., Zhu, X. X., Moorefield, C. N., Kotta, K., & Newkome, G. R. (2007b). Effect of ionic binding on the self-diffusion of anionic dendrimers and hydrophilic polymers in aqueous systems as studied by pulsed gradient NMR techniques. *Macromolecules, 40*(10), 3644–3649.

Thérien-Aubin, H., Zhu, X. X., Ravenelle, F., & Marchessault, R. H. (2008). Membrane formation and drug loading effects in high amylose starch tablets studied by NMR imaging. *Biomacromolecules, 9*, 1248–1254.

Tritt-Goc, J., Kowalczuk, J., & Pislewski, N. (2003). Magnetic resonance imaging study of the transport phenomena of solvent into the gel layer of hypromellose matrices containing tetracycline hydrochloride. *Journal of Pharmacy and Pharmacology, 55*(11), 1487–1493.

Veregin, R. P., Fyfe, C. A., Marchessault, R. H., & Taylor, M. G. (1986). Characterization of the crystalline A and B starch polymorphs and investigation of starch crystallization by high-resolution ^{13}C CP/MAS NMR. *Macromolecules, 19*, 1030–1034.

Whistler, R. L., BeMiller, J. N., & Paschall, E. F. (1984). *Starch: Chemistry and technology*. Orlando: Academic Press.

Wu, H.-C. H., & Sarko, A. (1978a). Packing analysis of carbohydrates and polysaccharides. IX. The double-helical molecular structure of crystalline A-amylose. *Carbohydrate Research, 61*, 27–40.

Wu, H.-C. H., & Sarko, A. (1978b). Packing analysis of carbohydrates and polysaccharides. VIII. The double-helical molecular structure of crystalline B-amylose. *Carbohydrate Research, 61*, 7–25.

Zhang, Y., Xiao, C., Bindzus, W., & Green, V. (2006). Tablet excipient based on starch. US Patent Office, Pat. No. US 2006/008521.

Ziegler, G. R., MacMillan, B., & Balcom, B. J. (2003). Moisture migration in starch molding operations as observed by magnetic resonance imaging. *Food Research International, 36*(4), 331–340.